



## Investigation of the cationic resin Amberlite®IRC-50 as a potential adsorbent to remove the anionic dye methyl orange

Jaouad Bensalah\*, Amar Habsaoui, Ahmed Lebki, Omar El Khattabi, El Housseine Rifi

Laboratory of Advanced Materials and Process Engineering, Department of Chemistry, Faculty of Sciences, Ibn Tofail University, B.P. 133, 14000 Kenitra, Morocco, emails: bensalahjaouad11@gmail.com (J. Bensalah), habsaoui.amar@uit.ac.ma (A. Habsaoui), lebkiarahm@yahoo.fr (A. Lebki), elkhattabi@uit.ac.ma (O. El Khattabi), elhosseinr@yahoo.fr (E. Housseine Rifi)

Received 24 July 2021; Accepted 10 November 2021

### ABSTRACT

The cationic exchange resin Amberlite®IRC-50 was evaluated as a potential adsorbent for toxic methyl orange (MO) dye. The adsorption study was evaluated as a function of time, temperature, pH value, optimal concentration of the anionic dye MO and adsorbent the cationic resin. The maximum retained content of MO was 68.2 mg g<sup>-1</sup> of concentration 200 mg L<sup>-1</sup>. The various values of the rate constant for adsorption process of the dye MO were determined. Kinetic analysis of the adsorption study of the impact of the concentration was compatible with linear pseudo-second-order (The experimental capacity is very close as the capacity calculates, 68.2 mg g<sup>-1</sup> of experimental capacity and 76.9 mg g<sup>-1</sup> of capacity calculates). The thermodynamic parameters  $\Delta G^\circ$  (-1.84 at -4.00 kJ mol<sup>-1</sup>),  $\Delta H^\circ$  (19.62 kJ mol<sup>-1</sup>) and  $\Delta S^\circ$  (72.00 kJ mol<sup>-1</sup>) were determined using the Van't Hoff equation. The values of these parameters indicate that the adsorption process is an endothermic and spontaneous. The adsorption process fit well with the Langmuir adsorption isotherm model.

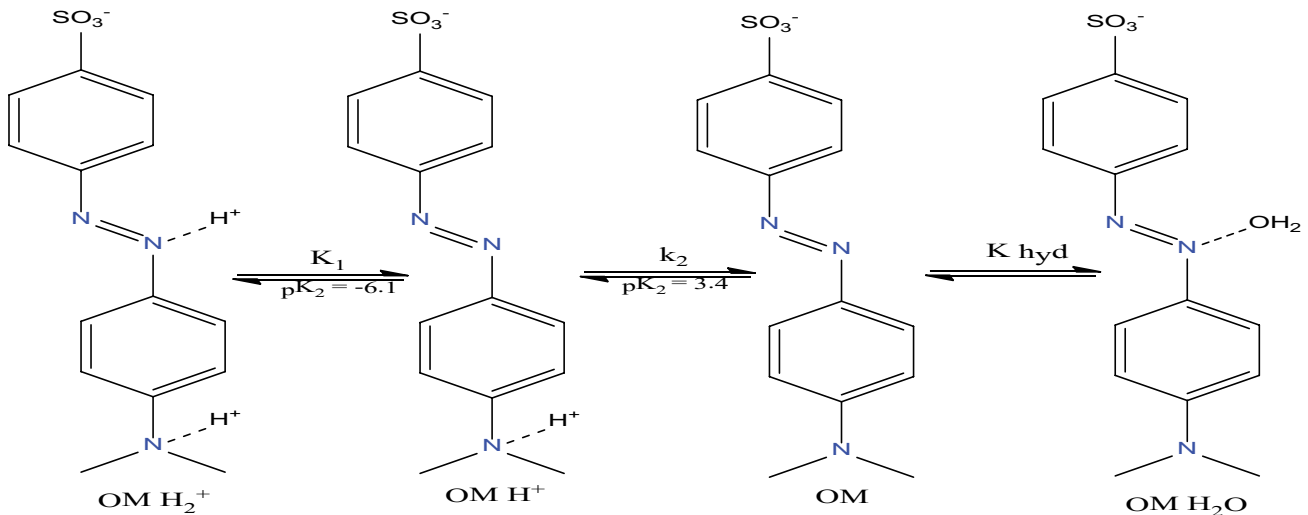
*Keywords:* Adsorption; Methyl orange; Ion exchange; Cationic resin; Langmuir model; Kinetic modeling

### 1. Introduction

Water pollution is among the most difficult problems for humanity. Among the main contributors to water pollution are dyes. As they are immediately released to water stream from several industries like for instance textiles, pith mills, food and lacing. Dyes are congregation fragrant molecules with a fierce color and high stability and non-biodegradable, this makes their elimination tedious [1,2]. Orange methyl is an anionic dye broadly utilized in the laboratory and in the fabric manufacture [3]. Cancer-causing and mutagenic. It is a powerful water pollutant [4,5]. In addition, wastewater laden with dyes is usually subjected to treatment by chemical processes. Conventional remedy methods such as curdling and flocculating [6,7], reverse

osmosis [8], the chemical oxidation and the ozonation [9–11], biological treatments [12], photo degradation [13], filtration through membranes [14–16], and adsorption [17], were developed for the drug of wastewater comprising dyes. Among the different processing technologies. The procedure of adsorption is very popular due to its rusticity, low cost and high effectiveness, may as well the ready-made of a wide range of extraction. The adsorption can be a best effectiveness to treat textile effluents since adsorbent of the cationic resin has many pleasant characteristics such as chemical. Thermal stability and specific acute surface. Organic ion exchange resins of the cationic resin appear more appropriate for removing poisonous elements due to their speedy kinetics, simple regeneration and uplift of the exchange capacity [18].

\* Corresponding author.



In this work adjusts to check the adsorption potential of a cationic resin, using the artificial Amberlite®IRC-50 in the form of beads in order to adsorb an anionic dye. For this purpose, the cationic resin which purchased by the company Sigma Aldrich. The cationic resin biopolymer was selected as a potential adsorbent to eliminate the dye methyl orange (MO) from an aqueous solution. In the adsorption study, the impacts of the cationic resin, temperature, adsorption time, dye optimal concentration and the pH. The mass transfer mechanism has been also studied. The isotherms were constructed at several various temperatures (298–328 K) and the curves were adjusted with the models of Freundlich and Langmuir Thermodynamics was estimated by ( $\Delta H^\circ$ ), ( $\Delta G^\circ$ ) and ( $\Delta S^\circ$ ). A rejuvenation study was carried out to assessment the potential for reuse of the adsorbents. The suggested adsorbent of the cationic resin has been examined of treat simulated textile pollutant.

## 2. Experimental

### 2.1. Materials

As adsorbent, we used a microporous cationic resin in the form of synthesized beads used with the crude formula  $C_{23}H_{37}Cl_2N_3O$  and the molar mass is  $442.5 \text{ g mol}^{-1}$ . Before its use as an adsorbent, it was first brought into contact with a 1.0 M HCl solution then several cycles of washing with distilled water for purification and neutralization purpose.

### 2.2. Preparation of solutions

The anionic dye MO ( $C_{14}H_{14}N_3O_3S^-Na^+$ ) of the molar mass is  $327.32 \text{ g mol}^{-1}$ , has been widely utilized to emulate organic pollutants by the laboratory of wastewater [19–22], and has been utilized as objective water pollutant. The elimination rate of the orange methyl was studied as the percentage of decrease by adsorbent. Solution of MO was contagious by dissolving  $1,000 \text{ mg L}^{-1}$  in distilled water. Also the dye MO is colored indicator used primarily for printing the coloring of textiles it has two protonation sites at nitrogen atoms (see diagram).

### 2.3. Methods

The investigation experiments were bearer out as a function of time ( $0 < t < 5 \text{ h}$ ), pH value ( $2 < \text{pH} < 11$ ), the mass of the cationic resin ( $0.05 \text{ g} < m < 2 \text{ g}$ ), the thermodegree ( $25^\circ\text{C} < T < 55^\circ\text{C}$ ) and the concentration of dye ( $10 \text{ mg L}^{-1} < [C] < 200 \text{ mg L}^{-1}$ ). The tests were bearer out by shaking 0.1 g of the resin in 100 mL of the solution of the dye with a concentration of  $10 \text{ mg L}^{-1}$ . The colored solution was brought into contact with the adsorbent until the adsorption evenness was reached. The evolution absorbance of the colored solution was resulted using a UV/visible spectrometer (UV-2005 spectrophotometer) at the center CUAETI at Ibn Tofail University (Kenitra, Morocco). The measurements were carried out at a wavelength ( $\lambda$ ) of 468 nm which coincide to the greatest adsorbate of the anionic methyl orange dye. The unconsumed dye concentration was determined using a calibration curve prepared by a range of known MO concentrations.

The dye adsorption potential of the cationic resin  $Q_e$  ( $\text{mg g}^{-1}$ ) and the dye eliminated rate  $R$  (%) suitably by Eqs. (1) and (2), respectively.

$$Q_e = (C_0 - C_e) \times \frac{V}{m} \quad (1)$$

$$R(\%) = \frac{(C_0 - C_e)}{C_0} \times 100 \quad (2)$$

where  $C_0$ : the initial concentrations ( $\text{mg L}^{-1}$ );  $C_e$ : the equilibrium concentrations ( $\text{mg L}^{-1}$ );  $m$ : the mass of the support(g);  $V$ : volume of the dye (mL).

The kinetic study was carried out by running the adsorption as a function of time. Kinetic models pseudo-first-order and pseudo-second-order were utilized to assess the kinetics of the adsorption. While various models as Langmuir and Freundlich isotherms at the equilibrium adsorption were studied and the frameworks for isotherm model were determined. On the other hand, the variation in the concentration makes it possible to evaluate the

impact of this parameter on the adsorption phenomenon then to deduce the thermodynamic parameters.

### 3. Results and discussion

#### 3.1. Adsorption/coagulation study

The adsorption/coagulation capacity of the cationic resin for the anionic MO was appraised. The dye MO elimination percentages were determined based on the initial and final of the concentrations. For the time-dependent test, the initial concentration of the dye MO was  $10.0 \text{ mg L}^{-1}$ . The evolution of the absorbance of the colored solution was weighted using a UV-2005 spectrophotometer-type UV/visible spectrometer (CUAE2TI) at a wavelength that corresponded to the maximum adsorbent of MO solution ( $\lambda = 468 \text{ nm}$ ). About  $0.1 \text{ g}$  of the cationic resin was stirred in  $100 \text{ mL}$  of MO dye to ensure the maximum contact between the resin and the MO (Fig. 1). All tests were performed at crystallizing temperature. After a certain interval of time, the summer dye eliminates until contact time.

#### 3.2. Kinetic study

In order to determine the time necessary to reach the adsorption equilibrium of the anionic dye (MO) on the cationic resin, the kinetic curve was constructed up to  $300 \text{ min}$ . The simultaneous evolution of the pH values and of the adsorption capacity  $Q_e$  of the dye MO by the resin beads as be operative of time is manifest in (Fig. 2). The adsorption was evaluated at constant mass optimal of adsorbent ( $0.1$ ),  $V$  of a  $100.0 \text{ mL}$ , and at  $T$  equal to  $25^\circ\text{C}$ .

It was found that the equilibrium was reached at  $120 \text{ min}$  as shown in Fig. 2. It was noticed a rapid adsorption occurs in the first  $50 \text{ min}$  direct by approve weak backward adsorption rate and the equilibrium reached at around  $120 \text{ min}$ . But in order to check the balance of the system, the contact time was continued to  $300 \text{ min}$  approbating to this kinetic contour, the adsorption sites were progressively occupied by the molecules dye MO. The top-most adsorption capacity, Approbating to Fig. 2 was about  $8.10 \text{ mg g}^{-1}$  of the MO dyes.

It appears from the obtained curve that the fixing capacity of the support by MO dye, growing with the growing in the contact time of Amberlite®IRC-50 with the colored solution of MO, thereafter beyond  $t = 120 \text{ min}$  a level of equilibrium is reached corresponding to the saturation of the spot where the maximum capacity obtained at approximately

$Q_{\text{max}} = 8.1 \text{ mg g}^{-1}$ . This extend in the adsorption amplitude of MO is accompanied by a lessening in the pH values which goes from  $6.5$  to  $2.1$  of the MO.

#### 3.3. Effect of the cationic resin mass on MO adsorption

To optimize the mass of the cationic resin for MO elimination, the study was carried out using various masses of the resin in the form of beads ranging from  $0.05$  to  $2 \text{ g}$ , each one of them was added to a in  $100.0 \text{ mL}$  of the colored solution at a concentration of  $10.0 \text{ mg L}^{-1}$  of MO and at a pH of  $6.5$ . The system is stirred at  $25^\circ\text{C}$  for  $5 \text{ h}$ .

The evolution of the removal yield of methyl orange as a function of the mass of the cationic resin is represented in Fig. 3.

The results obtained see that the equilibrium time decreases as the mass of the adsorbent increases, which may be due to the study of variations in the percentage of elimination of methyl orange as a function of time adsorbent dose in parallel with the increase in mass of the cationic resin from  $0.05$  to  $2 \text{ g}$ . The curves in Fig. 3 show that the percentage of elimination of the MO dye practically reached of total a  $100\%$  for a mass of  $2.0 \text{ g}$  of the resin. These results reveals that, the increase in the mass of the adsorbent increases the number of adsorption sites available for trapping the dye, which consequently favors the discoloration process of the studied aqueous solution [23].

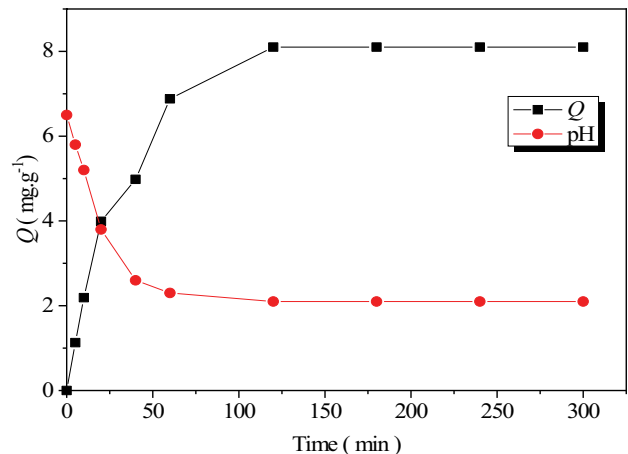


Fig. 2. Evolution of pH and MO adsorption capacity by the cationic resin as a function of time and pH value using a solution MO with  $10 \text{ mg L}^{-1}$  concentration,  $T$  of  $25^\circ\text{C}$  and  $V$  of  $100 \text{ mL}$ .

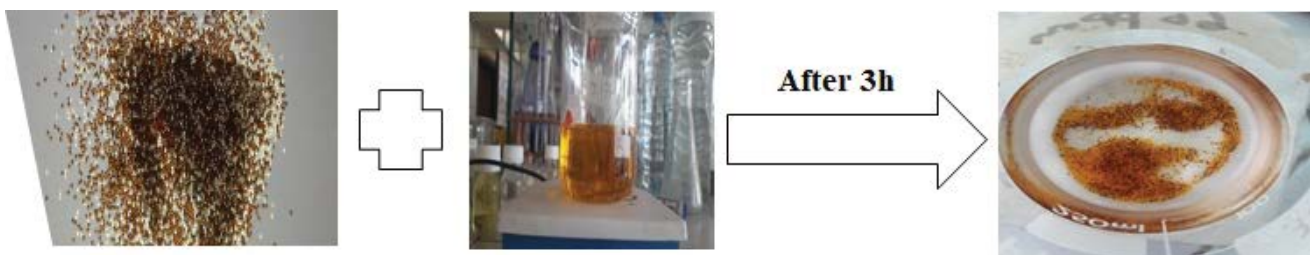


Fig. 1. Adsorption of the MO dye using on the cationic resin.

Indeed, a mass of 0.1 g of the cationic resin gave an extraction rate of adsorption of about 80.20%, this value was chosen as the optimal mass for economic reasons.

3.4. Effect of pH on the adsorption of the methyl orange dye

The pH is paramount source that affects the adsorption process; in order to it influences the exterior charge of the adsorbent and the ionization of the cationic resin. Fig. 4 reveals that the change in pH from 2.0 to 11 produced an increase in the percentage of dye elimination. From Fig. 4, the greatest pH for the following adsorption experiments was procured. For all dye solutions, the percentage of removal was elevation under acidic conditions, the molecules of MO in anionic form involved with hydrogen ions in aqueous solution for the adsorption sites, by lessening the

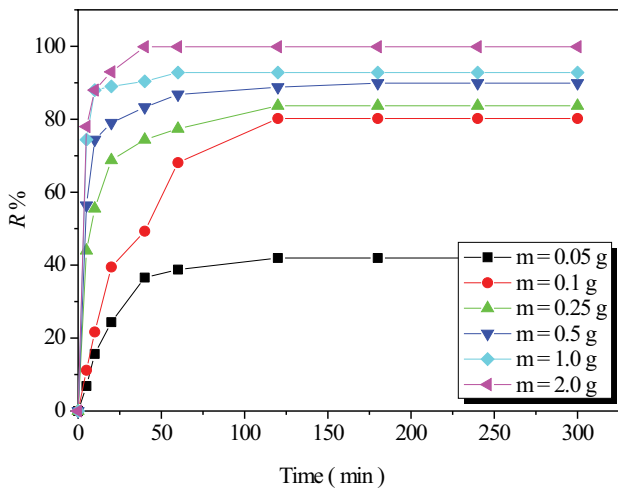


Fig. 3. Adsorption efficiency of MO by various masses of the cationic resin a pH = 6.5, [MO] = 10 mg L<sup>-1</sup>, T = 25°C and V = 100.0 mL.

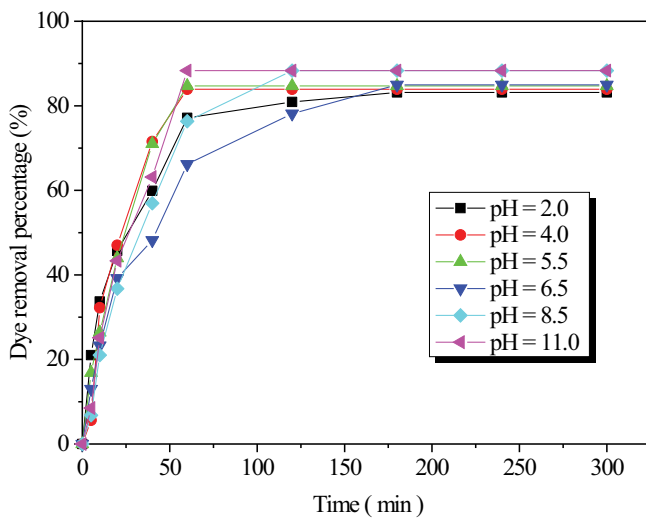


Fig. 4. The percentage of MO removal as a function of time at various pH values,  $m = 0.1$  g,  $V = 100$  mL, and  $[MO] = 10.0$  mg L<sup>-1</sup>,  $T = 298$  K.

adsorption. In this way, electrostatic interaction can occur between the charged resin and the charged dyes as well.

3.5. Effect of temperature

In order to straighten the effect of temperature on the adsorption capacity of the cationic resin for the dye MO, a 0.1 g of the cationic resin was added to a 100 mL solution of the anionic dye MO, adsorption studies were transmit out at various temperature ranging from 25°C up to 55°C (Fig. 5). The adsorption capacities of MO on the cationic resin increased by growing the temperature, which indicates that the adsorption of MO on the resin from an aqueous solution could be an endothermic process [24].

3.6. Effect of initial concentration of MO on rate of adsorption

The adsorption of MO by the cationic resin was also studied as a function of primary concentrations of the anionic dye MO (10, 20, 40, 100 and 200 mg L<sup>-1</sup>). Fig. 6 and Table 1 show the adsorption results as a function of the two variables time and primary concentration. As can be seen from Fig. 6, the quantity of MO adsorbed at low initial concentration (10 mg L<sup>-1</sup>) reaches the adsorption saturation at 120 min, also, as for the concentrations of MO (100 mg L<sup>-1</sup>), the time necessary to reach equipoise was also about 120 min.

It is noted from the obtained curve (Fig. 6), a rapid increase in the MO extraction capacity by the cationic resin

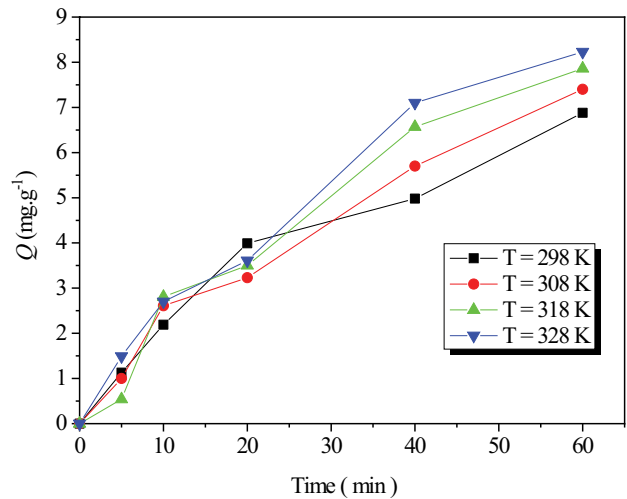


Fig. 5. Variation of the percentage of elimination of MO as a function of time at various temperature values,  $m_{\text{using}} = 0.1$  g, pH = 6.5,  $V = 100$  mL, and  $[MO] = 10$  mg L<sup>-1</sup>.

Table 1

Evolution of the anionic MO retention capacity on the cationic resin beads as a function of initial concentration of MO, ( $m$  of dry resin = 0.1 g,  $V = 100$  mL, pH = 6.5,  $T = 25^\circ\text{C}$ )

[MO] mg L <sup>-1</sup>	10	20	40	100	200
$Q_m$ (mg g <sup>-1</sup> )	8.1	18.59	36.14	59.48	68.2
R (%)	80.20	79.73	79.11	60.55	36.05

depending on the initial concentration of MO, a concentration over  $100 \text{ mg L}^{-1}$  of the dye, a plateau corresponding to the saturation of the support reached at  $Q_{\text{max}} = 68.2 \text{ mg g}^{-1}$ . This result can be associated to an growing in the leadership force of the concentration gradient [25].

Table 1 shows that the increase in the initial concentration of MO dye results in growing in the adsorption of the methyl orange dye MO. In fact, the adsorption capacity increased from  $8.1$  to  $68.2 \text{ mg g}^{-1}$  for MO concentrations growing from  $10$  to  $200 \text{ mg L}^{-1}$  respectively. However, the dye elimination rate decreased from  $80.2\%$  to  $36.05\%$ .

### 3.7. Kinetic adsorption models

The adsorption kinetics is evaluated utilized pseudo-first-order and pseudo-second-order in order to definite the

mechanism of the adsorption of methyl orange MO on the cationic resin.

#### 3.7.1. First-order model

The pseudo-first-order equation is given by Eq. (3).

The values of the pseudo-first-order rate constants,  $k_1$  and  $q_e$  were determined from the sloped and intercepts of the log plots  $(q_e - q_t)$  with  $t$ , respectively, results are listed in Table 2. If the  $q_e$  values determined from this model rate is in agreement with the capacity experimental values, this indicates that adsorption follows the first-order kinetic model.

Plots of  $\log(q_e - q_t)$  with time are shown in Fig. 7, the plotting was performed for results obtained from various initial concentrations. Experimental kinetics data

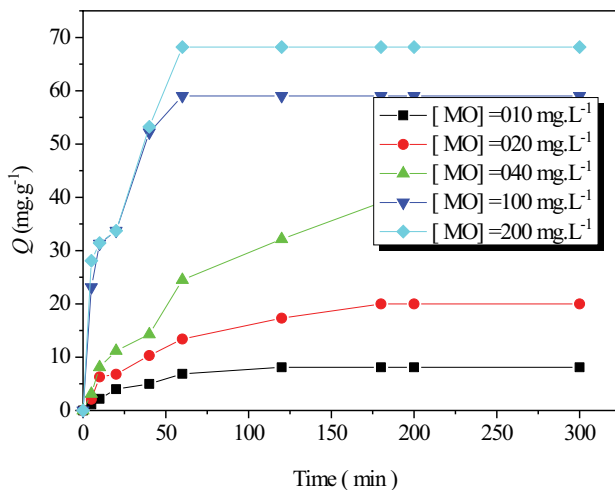


Fig. 6. Effect of the concentration on the adsorption of MO ( $m = 0.1 \text{ g}$ ,  $\text{pH} = 6.5$ ,  $V = 100 \text{ mL}$ ,  $T = 298 \text{ K}$ ).

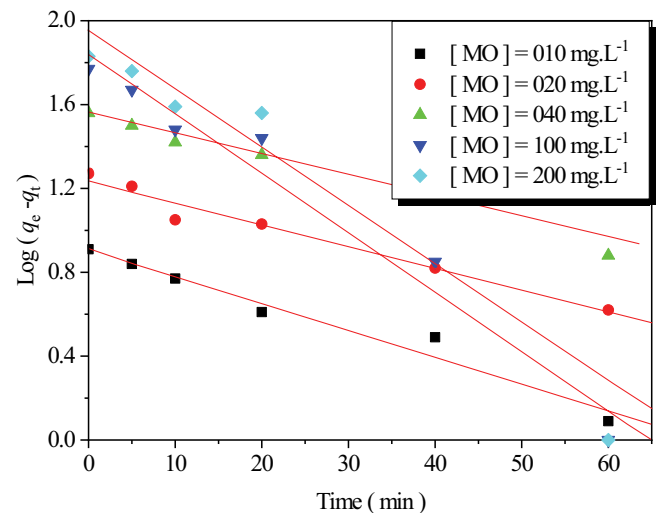


Fig. 7. Kinetic pseudo-first-order model of MO adsorption on the cationic resin beads.

Table 2

Parameters of the kinetic model of the pseudo-first-order and the pseudo-second-order of the MO

Kinetic model	[MO] $\text{mg L}^{-1}$	$q_{e\text{-exp}}$ ( $\text{mg g}^{-1}$ )	$q_{e\text{-cal}}$ ( $\text{mg g}^{-1}$ )	$k_1$ ( $\text{min}^{-1}$ )	$R^2$
Pseudo-first-order	10	8.1	8.05	0.03	0.980
	20	18.59	16.98	0.023	0.985
	40	36.14	36.30	0.022	0.946
	100	59.48	69.18	0.064	0.982
	200	68.2	87.09	0.062	0.942
Pseudo-second-order	10	8.1	9.09	0.058	0.992
	20	18.59	20.40	0.042	0.991
	40	36.14	41.66	0.024	0.970
	100	59.48	62.50	0.037	0.999
	200	68.2	76.92	0.026	0.999

Note that the value of  $R^2$  of the line of best fit using the pseudo-second-order of the kinetic equation is 0.999, the calculated adsorption capacity ( $q_{e\text{-cal}}$ ) was  $9.09$  to  $76.92 \text{ mg g}^{-1}$ . The experimental adsorption amplitude ( $q_{e\text{-exp}}$ ) by pseudo-second-order was  $8.1$  to  $68.2 \text{ mg g}^{-1}$ , these values are very close to that measured experimentally, indicating an the cationic resin lead with adsorption of the anionic dye (MO) in accordance with the pseudo-second-order kinetics. In pseudo-first-order (Fig. 7), the value of  $R^2$  for the line of best fit is 0.94. The theory of calculated equilibrium adsorption capacity ( $q_{e\text{-cal}}$ ) of  $87.09 \text{ mg g}^{-1}$  is far from that measured experimentally ( $q_{e\text{-exp}}$ ,  $68.2 \text{ mg g}^{-1}$ ), indicating that the kinetics of adsorption can be characterized as a pseudo-second-order. We can thence conclude that physisorption is the flow control step for the adsorption of the anionic dye MO on the surface of the cationic resin beads.

were modeled by the pseudo-first-order kinetic model and pseudo-second-order kinetic models [24,25].

$$\log(q_e - q_t) = \log(q_e) - \left(\frac{k_1}{2.203}\right) \cdot t \quad (3)$$

where  $q_t$  (mg g<sup>-1</sup>) is the adsorption quantity of organic MO dye at each instant  $t$ ,  $q_e$  (mg g<sup>-1</sup>) is the adsorption capacity at equilibrium and  $k_1$  (min<sup>-1</sup>) is the pseudo-first-order velocity constant. Knowing that  $k_1$  and we calculated from the slopes and extrapolations of logarithmic plots ( $q_e - q_t$ ) with respect to time to which are listed in Table 2. The variation of the pseudo-first-order is given according to Fig. 7:

### 3.7.2. Second-order model

The pseudo-second-order kinetic model is obvious in linear form as seen in Eq. (4).

The values of  $q_e$  and  $k_1$  can be obtained from the inclination and the intercepts, respectively of the  $t/q_t$  vs.  $t$  curves (Fig. 8), results are summarized in Table 2. The theoretical results didn't correlate with the experimental with this model [24,25].

$$\frac{t}{q_t} = \frac{1}{k_2 q_e^2} + \frac{1}{q_e} \times t \quad (4)$$

where  $k_2$  is the pseudo-second-order constant (g mol<sup>-1</sup> min<sup>-1</sup>) and  $q_e$  (mg g<sup>-1</sup>) is the adsorption capacity at equilibrium. The lines in Fig. 8 represent the variation of Eq. (4) as a function of time.

### 3.8. Adsorption isotherm

The adsorption isotherm provides importance valuable acquaintance on the way the dye molecules are distributed between the aqueous solution and the adsorbent at equilibrium state, which is essential for optimizing the amount of the cationic resin. Three adsorption isotherms were examined in the present study Langmuir and Freundlich.

Experimental kinetics data were modeled by the Freundlich and Langmuir models [26–28].

#### 3.8.1. Langmuir adsorption isotherm

The basic hypothesis of the Langmuir is that adsorption takes place at specified homogeneous sites within the cationic resin [26]. The results of the adsorption tests of the anionic dye MO on the cationic resin were processed by the Langmuir model represented by Eq. (5).

$$\frac{C_e}{Q_e} = \frac{C_e}{Q_m} + \frac{1}{(K_L \times Q_m)} \quad (5)$$

where  $C_e$  is equilibrium concentration (mg L<sup>-1</sup>),  $Q_m$ : adsorption capacity (mg g<sup>-1</sup>) and  $K_L$ : Langmuir equilibrium constant (L mg<sup>-1</sup>).

The values of  $Q_{max}$  and  $K_L$  are determined from the intersection with the ordinate axis and the slope of the line  $C_e/Q_e = f(C_e)$  (Fig. 9).

At a given temperature, the free enthalpy of adsorption  $\Delta G^\circ_{ads}$  (kJ mol<sup>-1</sup>) can be calculated by Eq. (6).

$$K_L = \frac{Q_e}{C_e} \quad (6)$$

$$\Delta G^\circ_{ads} = -R \times T \ln(\rho \times K_L) \quad (7)$$

where  $R$ ,  $T$  and  $K_L$ , respectively represent the constant of the ideal gases, and  $\rho_{MO} = 1.28$  g cm<sup>-3</sup> is the density of the solution of MO, the absolute temperature and the Langmuir constant. The calculated free enthalpy of adsorption is given in Table 3.

#### 3.8.2. Freundlich adsorption isotherm

The Freundlich isotherm presume that, the adsorption is multilayer and that the surface of the cationic resin is heterogeneous [27,28]. The linear form of Freundlich equation can be expressed.

$$\log(q_e) = \log(K_F) + \frac{1}{n} \times \log(C_e) \quad (8)$$

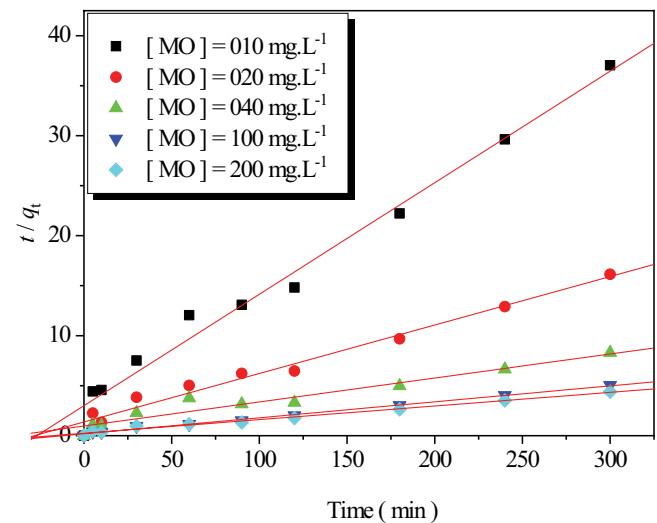


Fig. 8. Kinetic pseudo-second-order model of MO adsorption on the cationic resin.

Table 3  
Parameter obtained from applying the Langmuir and Freundlich models

Langmuir	$Q_{m-exp}$ (mg g <sup>-1</sup> )	$Q_{m-cal}$ (mg g <sup>-1</sup> )	$K_L$ (L mg <sup>-1</sup> )	$\Delta G^\circ$ (kJ mol <sup>-1</sup> )	$R^2$
	68.2	76.92	0.094	-5.86	0.998
Freundlich	$1/n$	$n$	$K_F$ (L mg <sup>-1</sup> )		$R^2$
	0.43	2.32	10.47		0.92

where  $K_f$  is Freundlich parameter ( $L\ mg^{-1}$ ) and  $n$  is heterogeneity index.

The value of  $K_f$  decreased by increasing the temperature, showing an endothermic nature of the adsorption process.

The values of  $K_f$  and  $n$  gated from the slope and the ordinate at the origin of the  $\log(q_e)$  vs.  $\log(C_e)$  are offered in Table 3,  $n = 2.32 > 1$ . So the results obtained using this model confirms the results obtained in the kinetic study.

As shown in Table 3, the Langmuir isotherm corresponds fairly well to the experimental data ( $R^2 > 0.98$ ). The monolayer adsorption capacity conformity to this model was  $76.92\ mg\ g^{-1}$  for the MO. This calculated value is close to the value of the maximum experimental adsorption capacity, exp values with small relative difference of about 7.83%.

### 3.9. Thermodynamic studies

Thermodynamic parameters, inclusive change in Gibbs free energy ( $\Delta G^\circ$ ), in enthalpy ( $\Delta H^\circ$ ) and in entropy ( $\Delta S^\circ$ ), are used to assess the impact of temperature on the adsorption of the dye MO on the cationic resin and prepared detailed information concerning the ingrained energy changes associated with the process [29].

The enthalpy ( $\Delta H^\circ$ ) and entropy ( $\Delta S^\circ$ ) parameters were predestined from classical relations:

$$\ln(K_L) = \left( \frac{\Delta S}{R} \right) - \left( \frac{\Delta H}{RT} \right) \quad (9)$$

$$\Delta G_{ads}^0 = \Delta H - T\Delta S \quad (10)$$

The curve of  $\ln(K_L)$  with respect to  $1/T$  gave a upright line shown in Fig. 10, and the various values of  $\Delta H^\circ$  ( $kJ\ mol^{-1}$ ) and  $\Delta S^\circ$  ( $kJ\ mol^{-1}$ ) were studied from the intersection and the slope of the equation of Van't Hoff plots, respectively. The values of  $\Delta G^\circ$  ( $kJ\ mol^{-1}$ ) have been recalculated from  $\Delta H^\circ$  and  $\Delta S^\circ$  (Table 4). The positive values of  $\Delta H^\circ$  are indicative of an endothermic adsorption process, both  $\Delta H^\circ$  and  $\Delta S^\circ$ .

From the thermodynamic point of view, Evaluated of the adsorption was the standard values of Gibbs free energy ( $\Delta G^\circ\ kJ\ mol^{-1}$ ), enthalpy ( $\Delta H^\circ\ kJ\ mol^{-1}$ ) and entropy ( $\Delta S^\circ\ J\ mol^{-1}$ ). All the thermodynamic parameters have been grouped in Table 4. The negative values of  $\Delta G^\circ$  have indicated that adsorption is spontaneous and convenient process. The positive value of  $\Delta H^\circ$  confirmed that the adsorption of MO on the cationic resin was an endothermic process of this magnitude and proved that the studied mechanism of adsorption of MO by the beads of the cationic resin is a physical adsorption (physisorption) [29].

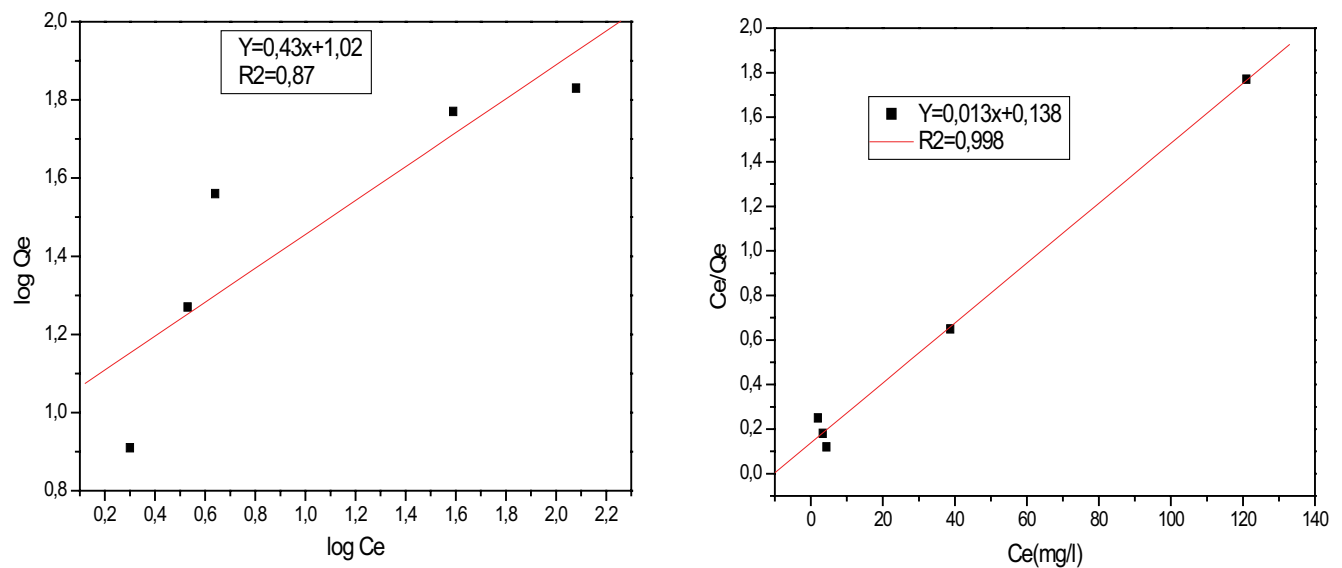
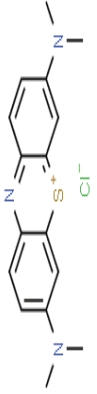
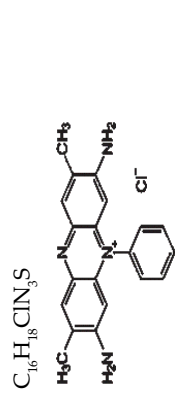
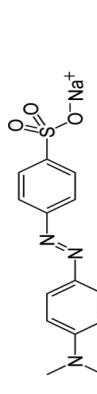
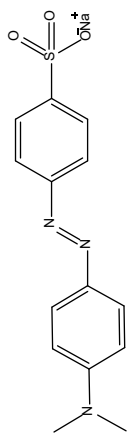
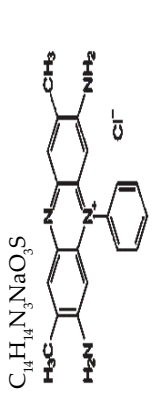


Fig. 9. Isothermal model of Freundlich and Langmuir for the adsorption of MO on the beads of the cationic resin.

Table 4  
Thermodynamic parameters

T (K)	1/T (K <sup>-1</sup> )	ln(K)	Q <sub>e</sub> (mg g <sup>-1</sup> )	C <sub>e</sub> (mg L <sup>-1</sup> )	ΔG° (kJ mol <sup>-1</sup> )	ΔH° (kJ mol <sup>-1</sup> )	ΔS° (kJ mol <sup>-1</sup> )
298	0.00335	0.96	6.88	3.22	-1.84		
308	0.00324	0.96	7.40	2.83	-2.56		
318	0.00314	1.38	7.88	1.97	-3.28	19.62	72.00
328	0.00304	1.43	8.23	1.97	-4.00		

Table 5  
Comparative study of dyes with our work

Dye type	Chemical structure and formula	Support	Result	References
Methylene blue (MB)	 $C_{16}H_{18}ClN_3S$	Elimination of the cationic methylene blue dye from aqueous solution utilized a superabsorbent hydrogel the polyacrylamide.	Efficiency of 90%; Adsorption equilibrium is reached after 540 min; $\Delta G^\circ$ (-4.94 at $-9.78 \text{ kJ mol}^{-1}$ ); $\Delta H^\circ$ (43.66 $\text{kJ mol}^{-1}$ ); $\Delta S^\circ$ (163.56 $\text{kJ mol}^{-1}$ ).	[32]
Safranin-T (SF) Methyl orange (MO)	 $C_{20}H_{19}ClN_4$	Studies on elimination of the cationic dye Safranin-T and the anionic dye methyl orange dyes using NaX zeolite synthesized from fly ash.	Elimination of dyes over the regenerated zeolites is only 68% whereas % removal of the anionic dye methyl orange on the fresh zeolite is 78%; Adsorption equilibrium is reached after 10 h of two dyes; $\Delta H^\circ$ (-20.18 $\text{kJ mol}^{-1}$ ); $\Delta S^\circ$ (-90.32 $\text{kJ mol}^{-1}$ ).	[33]
Crystal violet (CV)	 $C_{14}H_{14}N_3NaO_3S$	Surface modified laterite soil with an the anionic surfactant for the elimination of a the dye crystal violet.	Removal of dye over the regenerated is only 86%; ( $C_i$ (CV)) = 250 $\text{mg L}^{-1}$ .	[34]
Methyl orange (MO)	 $C_{25}H_{30}N_3$	Investigation of the cationic resin Amberlite®IRC-50 as a potential adsorbent to remove the anionic dye methyl orange.	Obtained results show the dye adsorption was rapid during the first few minutes and the rate of removal reached over 80.20%, in the first 90 min.	This work
Safranin-T (SF) Methylene blue (MB)	 $C_{20}H_{19}ClN_4$	Kinetic and thermodynamic study of the adsorption of cationic dyes by the cationic artificial resin Amberlite®IRC-50.	Concentration of 20 $\text{mg L}^{-1}$ for the two colorants MB and SF; Kinetic study also shows that equilibrium is reached after 120 and 180 min respectively for two solutions of the dyes MB and SF; Maximum absorption capacity of approximately 12.20 $\text{mg g}^{-1}$ for the MB dye and 13.30 $\text{mg g}^{-1}$ for the SF dye.	[35]



The enthalpy values  $\Delta H^\circ$  are positive, which seen that also the adsorption process of MO on the cationic resin is endothermic [30].

#### 4. Comparative study

Our work uses a support commercialized by Sigma Aldrich adsorption of the anionic dye methyl orange by cationic resin in the form of beads. This work focused on the elimination of the MO dye from aqueous solutions. The results obtained show that the adsorption of the dye was rapid pending the first minutes and that the rate of elimination reached over 97% during the first 50 min. Then, stabilized at 120 min of 0.1 g mass and concentration of 10 mg L<sup>-1</sup> and also the maximum capacity are 68.2 mg g<sup>-1</sup>

to 0.1 g of concentration 200 mg L<sup>-1</sup>, on the other hand, in another work with the same dye we find the maximum capacity less than our work with a good correlation of the seat of the  $R^2$  is 0.998 is better than the other work have been grouped in Table 5 [31].

#### 4.1. Adsorption mechanism

The possible interaction of the cationic resin with MO dyes is shown in Fig. 11. The adsorption mechanism is governed by various factors such as the structure and functional activity of the adsorbent molecules and specificity. Adsorbent molecules Surface point of the adsorbent. The adsorbent in this case is the dye molecule, which is flat and can be easily adsorbed onto the adsorbent through van

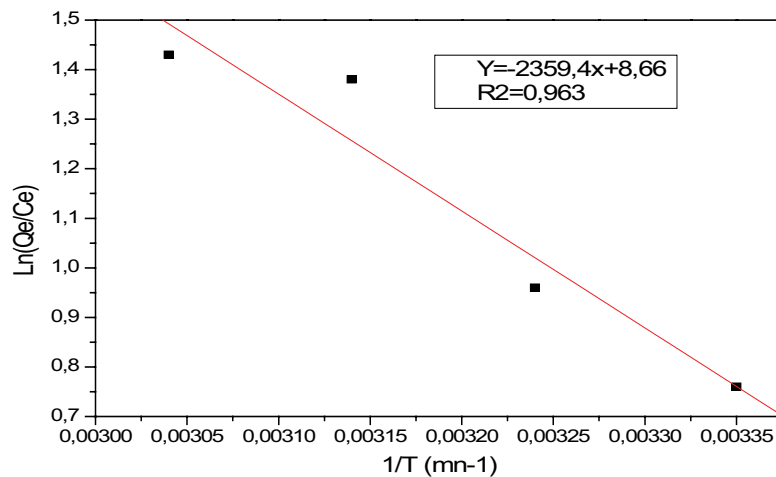


Fig. 10. The Van't Hoff curve of MO adsorption on the cationic resin.

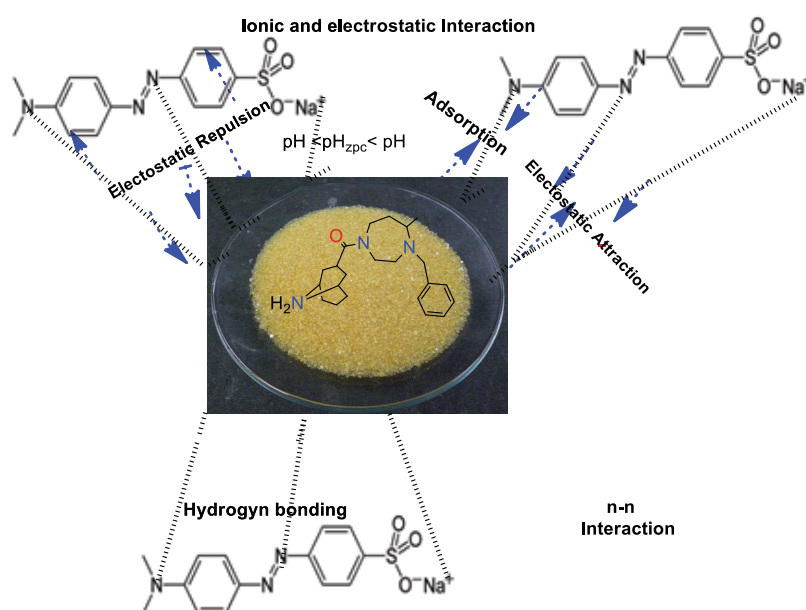


Fig. 11. Adsorption mechanism of methyl orange (MO) on the cationic resin Amberlite®IRC-50.

der Waals forces and cationic resin extra-cavity hydrogen bonding interactions. In the case of anionic dye, the force Electrostatic interactions play a role in the adsorption process.

However, the lower adsorption of the cationic resin suggests that its larger size and hydrophobic nature precludes any interaction with MO. On the other hand, the cationic MO dye can be bound to the cationic resin by electrostatic interactions, van der Waals forces and hydrogen bonds in addition to host-guest interactions with the resin cavity.

The higher carbon content after adsorption indicates that the dye has adsorbed successfully to the surface of the cationic resin. The presence of elements such as nitrogen and oxygen on the adsorbent + MO further demonstrates their presence on the adsorbent by the adsorption process. It can therefore be assumed that the change in the composition of the elements corresponds to the adsorption of the dye, possibly due to these possible interactions.

## 5. Conclusion

This study demonstrates the effectiveness of the cationic resin in removing the dye methyl orange from an aqueous medium. The effect of several parameters related to the adsorption efficiency such as contact time, adsorbent dose, pH value, initial concentration of the dye and temperature were evaluated. The kinetic study shows that equilibrium is established after 10, 20, 60 and 120 min for MO solutions at 10, 20, 100, 200 mg L<sup>-1</sup>, respectively and the adsorption mechanism can be described by pseudo-second-order kinetics. The plot of the adsorption isotherms shows that the Langmuir model perfectly represents the adsorption of MO on the resin with a maximal adsorption capacity of around 68.2 mg g<sup>-1</sup>. The obtained thermodynamic parameters indicate that, the adsorption of the methyl orange dye on the cationic resin is an endothermic process. From the obtained results, the cationic resin could be considered an effective adsorbent for MO dye, the adsorption process could have scaled to a commercial scale.

## References

- [1] R. Sharma, P.K. Kar, S. Dash, Efficient adsorption of some substituted styrylpyridinium dyes on silica surface from organic solvent media – analysis of adsorption-solvation correlation, *Colloids Surf., A*, 624 (2021) 126847, doi: 10.1016/j.colsurfa.2021.126847.
- [2] H. Hanafy, Adsorption of methylene blue and bright blue dyes on bayleaf capertree pods powder: understanding the adsorption mechanism by a theoretical study, *J. Mol. Liq.*, 332 (2021) 115680, doi: 10.1016/j.molliq.2021.115680.
- [3] L. Labiadh, A. Barbucci, M.P. Carpanese, A. Gadri, S. Ammar, M. Panizza, Comparative depollution of methyl orange aqueous solutions by electrochemical incineration using TiRuSnO<sub>2</sub>/BDD and PbO<sub>2</sub> as high oxidation power anodes, *J. Electroanal. Chem.*, 766 (2016) 94–99.
- [4] U. Habiba, T.A. Siddique, T.C. Joo, A. Salleh, B.C. Ang, A.M. Afifi, Synthesis of chitosan/polyvinyl alcohol/zeolite composite for removal of methyl orange, Congo red and chromium(VI) by flocculation/adsorption, *Carbohydr. Polym.*, 157 (2017) 1568–1576.
- [5] S. Chen, J. Zhang, C. Zhang, Q. Yue, Y. Li, C. Li, Equilibrium and kinetic studies of methyl orange and methyl violet adsorption on activated carbon derived from *Phragmites australis*, *Desalination*, 25 (2010) 149–156.
- [6] Z. Li, L. Sellaoui, D.S.P. Franco, M.S. Netto, J. Georjgin, G.L. Dotto, A. Bajahzar, H. Belmabrouk, A. Bonilla-Petriciolet, Q. Li, Adsorption of hazardous dyes on functionalized multiwalled carbon nanotubes in single and binary systems: experimental study and physicochemical interpretation of the adsorption mechanism, *Chem. Eng. J.*, 389 (2020) 124467, doi: 10.1016/j.cej.2020.124467.
- [7] Z. Li, H. Hanafy, L. Zhang, L. Sellaoui, M. Schadeck Netto, M.L.S. Oliveira, M.K. Selim, G. Luiz Dotto, A. Bonilla-Petriciolet, Q. Li, Adsorption of congo red and methylene blue dyes on an ashitaba waste and a walnut shell-based activated carbon from aqueous solutions: experiments, characterization and physical interpretations, *Chem. Eng. J.*, 388 (2020) 124263, doi: 10.1016/j.cej.2020.124263.
- [8] H. Hanafy, L. Sellaoui, P.S. Thue, E.C. Lima, G.L. Dotto, T. Alharbi, H. Belmabrouk, A. Bonilla-Petriciolet, A.B. Lamine, Statistical physics modeling and interpretation of the adsorption of dye remazol black B on natural and carbonized biomasses, *J. Mol. Liq.*, 299 (2020) 112099, doi: 10.1016/j.molliq.2019.112099.
- [9] L. Zhang, L. Sellaoui, D. Franco, G.L. Dotto, A. Bajahzar, H. Belmabrouk, A. Bonilla-Petriciolet, M.L.S. Oliveira, Z. Li, Adsorption of dyes brilliant blue, sunset yellow and tartrazine from aqueous solution on chitosan: analytical interpretation via multilayer statistical physics model, *Chem. Eng. J.*, 382 (2020) 122952, doi: 10.1016/j.cej.2019.122952.
- [10] Y.L. de O. Salomón, J. Georjgin, D.S.P. Franco, M.S. Netto, E.L. Foletto, D.G.A. Picilli, L. Sellaoui, G.L. Dotto, Transforming pods of the species *Capparis flexuosa* into effective biosorbent to remove blue methylene and bright blue in discontinuous and continuous systems, *Environ. Sci. Pollut. Res. Int.*, 28 (2021) 8036–8049.
- [11] H.A.A. Yousef, B.M. Alotaibi, M.M. Alanazi, F. Aouaini, L. Sellaoui, A.B. Petriciolet, Theoretical assessment of the adsorption mechanism of ibuprofen, ampicillin, orange Gand malachite green on a biomass functionalized with plasma, *J. Environ. Chem. Eng.*, (2020) (In Press), doi: 10.1016/j.jece.2020.104950.
- [12] H.A.M. Saleh, I. Mantasha, K.M.A. Qasem, M. Shahid, M.N. Akhtar, M.A. AlDamen, M. Ahmad, A two dimensional Co(II) metal-organic framework with *bee* topology for excellent dye adsorption and separation: exploring kinetics and mechanism of adsorption, *Inorg. Chim. Acta*, 512 (2020) 119900, doi: 10.1016/j.ica.2020.119900.
- [13] P. Sirajudheen, S. Meenakshi, Encapsulation of Zn-Fe layered double hydroxide on activated carbon and its litheness in tuning anionic and rhoda dyes through adsorption mechanism, *Asia-Pac. J. Chem. Eng.*, 15 (2020) e2479, doi: 10.1002/apj.2479.
- [14] F. Dhaouadi, L. Sellaoui, G.L. Dotto, A. Bonilla-Petriciolet, A. Erto, A.B. Lamine, Adsorption of methylene blue on comminuted raw avocado seeds: interpretation of the effect of salts via physical monolayer model, *J. Mol. Liq.*, 305 (2020) 112815, doi: 10.1016/j.molliq.2020.112815.
- [15] T.D. Pham, T.T. Tran, V.A. Le, T.T. Pham, T.H. Dao, T.S. Le, Adsorption characteristics of molecular oxytetracycline onto alumina particles: the role of surface modification with an anionic surfactant, *J. Mol. Liq.*, 287 (2019) 110900, doi: 10.1016/j.molliq.2019.110900.
- [16] D. Kaner, A. Saraç, B.F. Şenkal, Removal of dyes from water using crosslinked aminomethane sulfonic acid based resin, *Environ. Geochem. Health.*, 32 (2010) 321–325, doi: 10.1007/s10653-010-9304-z.
- [17] (a) I. Mantasha, M. Shahid, H.A.M. Saleh, K.A.M. Qasem, M. Ahmad, A novel sustainable metal organic framework as the ultimate aqueous phase sensor for natural hazards: detection of nitrobenzene and F<sup>-</sup> at the ppb level and rapid and selective adsorption of methylene blue, *CrystEngComm*, 22 (2020) 3891–3909. (b) K. Iman, M. Shahid, M. Ahmad, A novel self-assembled Na{Cu<sub>12</sub>Zn<sub>4</sub>} multifunctional material: first report of a discrete coordination compound for detection of Ca<sup>2+</sup> ions and selective adsorption of cationic dyes in water, *Dalton Trans.*, 49 (2020) 3423–3433.

- [18] J. Bensalah, M. Berradi, A. Habsaoui, M. Allaoui, Kinetic and thermodynamic study of the adsorption of cationic dyes by the cationic artificial resin Amberlite®IRC50, *Mater. Today: Proc.*, 45 (2021) 7468–7472.
- [19] M.M. Khan, J. Lee, M.H. Cho, Au@TiO<sub>2</sub> nanocomposites for the catalytic degradation of methyl orange and methylene blue: an electron relay effect, *J. Ind. Eng. Chem.*, 20 (2014) 1584–1590.
- [20] X. An, C. Gao, J. Liao, X. Wu, X. Xie, Synthesis of mesoporous N-doped TiO<sub>2</sub>/ZnAl-layered double oxides nanocomposite for efficient photodegradation of methyl orange, *Mater. Sci. Semicond. Process.*, 34 (2015) 162–169.
- [21] D. Ljubas, G. Smoljanić, H. Juretić, Degradation of methyl orange and Congo Red dyes by using TiO<sub>2</sub> nanoparticles activated by the solar and the solar-like radiation, *J. Environ. Manage.*, 161 (2015) 83–91.
- [22] F.Z. Mahjoubi, A. Khalidi, A. Elhalil, N. Barka, Characteristics and mechanisms of methyl orange sorption onto Zn/Al layered double hydroxide intercalated by dodecyl sulfate anion, *Sci. Afr.*, 6 (2019) e00216, doi: 10.1016/j.sciaf.2019.e00216.
- [23] Y. Jun, S. Lee, K. Lee, M. Choi, Effects of secondary mesoporosity and zeolite crystallinity on catalyst deactivation of ZSM-5 in propanal conversion, *Microporous Mesoporous Mater.*, 245 (2017) 16–23.
- [24] J. El Gaayda, R.A. Akbour, F.E. Titchou, H. Afanga, H. Zazou, C. Swanson, M. Hamdani, Uptake of an anionic dye from aqueous solution by aluminum oxide particles: equilibrium, kinetic, and thermodynamic studies, *Groundwater Sustainable Dev.*, 12 (2021) 100540, doi: 10.1016/j.gsd.2020.100540.
- [25] J. Bensalah, A. Habsaoui, B. Abbou, L. Kadiri, I. Lebkiri, A. Lebkiri, E. Housseine Rifi, Adsorption of the anionic dye methyl orange on used artificial zeolites: kinetic study and modeling of experimental data, *Mediterr. J. Chem.*, 9 (2019) 311–316.
- [26] A. Dalalibera, P.B. Vilela, T. Vieira, V.A. Becegato, A.T. Paulino, Removal and selective separation of synthetic dyes from water using a polyacrylic acid-based hydrogel: characterization, isotherm, kinetic, and thermodynamic data, *J. Environ. Chem. Eng.*, 8 (2020) 104465, doi: 10.1016/j.jece.2020.104465.
- [27] M.H. Kanani-Jazi, S. Akbari, Amino-dendritic and carboxyl functionalized halloysite nanotubes for highly efficient removal of cationic and anionic dyes: kinetic, isotherm, and thermodynamic studies, *J. Environ. Chem. Eng.*, 93 (2021) 105214, doi: 10.1016/j.jece.2021.105214.
- [28] A. Raj, A. Yadav, A.P. Rawat, A.K. Singh, S. Kumar, A.K. Pandey, R. Sirohi, A. Pandey, Kinetic and thermodynamic investigations of sewage sludge biochar in removal of Remazol Brilliant Blue R dye from aqueous solution and evaluation of residual dyes cytotoxicity, *Environ. Toxicol. Chem.*, 23 (2021) 101556, doi: 10.1016/j.eti.2021.101556.
- [29] Z. Liu, G. Zhao, M. Brewer, Q. Lv, E.J.R. Sudhölter, Comprehensive review on surfactant adsorption on mineral surfaces in chemical enhanced oil recovery, *Adv. Colloid Interface Sci.*, 294 (2021) 102467, doi: 10.1016/j.cis.2021.102467.
- [30] G. Moussavi, R. Khosravi, The removal of cationic dyes from aqueous solutions by adsorption onto pistachio hull waste, *Chem. Eng. Res. Des.*, 89 (2011) 2182–2189.
- [31] V.S. Mane, I.D. Mall, V.C. Srivastava, Kinetic and equilibrium isotherm studies for the adsorptive removal of Brilliant Green dye from aqueous solution by rice husk ash, *J. Environ. Manage.*, 84 (2007) 390–400.
- [32] M. Ghaedi, S. Hajjati, Z. Mahmudi, I. Tyagi, S. Agarwal, A. Maity, V.K. Gupta, Modeling of competitive ultrasonic assisted removal of the dyes – Methylene blue and Safranin-O using Fe<sub>3</sub>O<sub>4</sub> nanoparticles, *Chem. Eng. Sci.*, 268 (2015) 28–37.
- [33] I. Lebkiri, B. Abbou, L. Kadiri, A. Ouass, Y. Essaadaoui, A. Habssaoui, E.H. Rifi, A. Lebkiri, Removal of methylene blue dye from aqueous solution using a superabsorbant hydrogel the polyacrylamide: isotherms and kinetic studies, *Mediterr. J. Chem.*, 9 (2019) 337–345.
- [34] S. Das, S. Barman, Studies on removal of Safranin-T and methyl orange dyes from aqueous solution using NaX zeolite synthesized from fly ash, *Int. J. Sci. Environ.*, 2 (2013) 735–747.
- [35] T.M.V. Ngo, T.H. Truong, T.H.L. Nguyen, T.T.A. Duong, T.H. Vu, T.T.T. Nguyen, T.D. Pham, Surface modified laterite soil with an anionic surfactant for the removal of a cationic dye (Crystal violet) from an aqueous solution, *Water Air Soil Pollut.*, 231 (2020) 285, doi: 10.1007/s11270-020-04647-2.